(3) Cowie, J. M. G.; McCrindle, J. T. *Eur. Polym. J.* **1972**, *8*, 1325.
(4) Cowie, J. M. G.; McEwen, J. J. *Macromolecules* **1974**, *7*, 291.
(5) Scornaux, J.; Van Leemput, R. *Makromol. Chem.* **1976**, *177*, 2721.
(6) Horta, A.; Fernández-Piérola, I. *Macromolecules* **1981**, *14*, 1519.
(7) Katime, I.; Strazielle, C. *Makromol. Chem.* **1977**, *178*, 2295.
(8) Maillols, H.; Bardet, L; Gromb, S. *Eur. Polym. J.* **1979**, *15*, 307.
(9) Gargallo, L; Radic, D.; Katime, I. *Eur. Polym. J.* **1981**, *17*, 439.
(10) Katime, I.; Ochoa, J. R.; Cesteros, L. C.; Peñafiel, J. *Polym. Bull.* **1982**, *6*, 429.
(11) Wenqing, Z.; Chengwei, X. *Fenzi. Kexue Xuebao* **1982**, *2*, 73.
(12) Fernández-Piérola, I.; Horta, A. *Makromol. Chem.* **1981**, *182*, 1705.
(13) Fernández-Martin, F.; Fernández-Piérola, I.; Horta, A. *J. Polym. Sci., Polym. Phys. Ed.* **1981**, *19*, 1353.
(14) Prolongo, M. G.; Masegosa, R. M.; Hernández-Fuentes, I.; Horta, A. *J. Phys. Chem.* **1984**, *88*, 000.
(15) Carr, C. J.; Zimm, B. H. *J. Chem. Phys.* **1950**, *18*, 1616.
(16) Huglin, M. B. "Light Scattering from Polymer Solutions"; Huglin, M. G., Ed.; Academic Press: London, 1972.
(17) Fernández-Piérola, I.; Horta, A. *J. Chim. Phys. Phys.-Chim. Biol.* **1980**, *77* (4), 271.
(18) Okita, K.; Teramoto, A.; Kawahara, K.; Fujita, H. *J. Phys. Chem.* **1968**, *72*, 278.
(19) Prolongo, M. G.; Masegosa, R. M.; Hernández-Fuentes, I.; Horta, A. *Polymer*, in press.
(20) Prolongo, M. G.; Masegosa, R. M.; Hernández-Fuentes, I.; Horta, A. *Macromolecules* **1981**, *14*, 1526.
(21) Masegosa, R. M.; Prolongo, M. G.; Hernández-Fuentes, I.; Horta, A. *Ber. Bunsenges. Phys. Chem.* **1984**, *88*, 103.
(22) Mehling, I. G.; Onken, U.; Arlt, W. "Vapor-Liquid Equilibrium Data Collection"; Dechema: 1978, Vol. I, Part 2b.
(23) Horta, A.; Prolongo, M. G.; Masegosa, R. M.; Hernández-Fuentes, *Polymer* **1981**, *22*, 1147.
(24) Read, B. E. *Trans. Faraday Soc.* **1960**, *56*, 382.
(25) Živný, A.; Pouchlý, J.; Šolc, K. *Collect. Czech. Chem. Commun.* **1967**, *32*, 2753.
(26) Katime, I.; Campos, A.; Teijón, J. M. *Eur. Polym. J.* **1979**, *15*, 291.
(27) Pouchlý, J.; Živný, A.; *J. Polym. Sci., Part A-2* **1972**, *10*, 1467.
(28) Tuzar, Z.; Bohdanecký, M. *Collect. Czech. Chem. Commun.* **1969**, *34*, 284.
(29) Horta, A.; Fernández-Piérola, I. *Polymer* **1981**, *22*, 783.
(30) Pouchlý, J.; Živný, A. *J. Polym. Sci., Part A* **1972**, *10*, 1481.
(31) Pouchlý, J.; Patterson, D. *Macromolecules* **1976**, *9*, 574.
(32) Horta, A. *Macromolecules* **1979**, *12*, 785.
(33) Flory, P. J. *Discuss. Faraday Soc.* **1970**, *49*, 7.
(34) Bondi, A. "Physical Properties of Molecular Crystals Liquid and Glasses"; Wiley: London, 1968.

Analysis of Stress-Induced Phase Separations in Polymer Solutions

Carlos Rangel-Nafaile,† Arthur B. Metzner,* and Kurt F. Wissbrun‡

Department of Chemical Engineering, University of Delaware, Newark, Delaware 19716.
Received May 5, 1983

ABSTRACT: The free energy of polymer solutions must depend upon the conformation of the macromolecules, and hence upon the deformation state imposed on the system, as well as upon the more familiar thermodynamic state variables of temperature and composition. As one consequence of the importance of this additional thermodynamic state variable, the precipitation temperature (cloud point) of polymer solutions may be increased by several tens of degrees Centigrade by imposition of steady shearing at low deformation rates. As a second consequence, the precipitated phase is sometimes found to be a solid of new morphology, and one which is quite refractory to re-solution. In this work a quantitative theoretical analysis of solubility phenomena in deforming solutions is given. The free energy of macromolecules in stagnant solutions is obtained from the Flory–Huggins theory, and changes with deformation state are computed from Marrucci's analysis for dilute solutions of elastic dumbbells. The parameters in the theoretical analysis were evaluated, using solutions of polystyrene in dioctyl phthalate, by measurements of the thermodynamic interaction parameter and of the rheological properties. The theory, which contains no adjustable parameters, was used to make a priori predictions of the change in cloud point with deformation state. The experimentally observed changes, of 3–28 °C, were predicted with a mean deviation of about 3 °C.

Introduction

Simple shear, when applied to materials, imparts both extension and rotation to a fluid element, under the influence of which polymer molecules will be oriented and stretched. In this way the distribution of the orientation and the end-to-end distance of the macromolecular coils will be modified, and such modifications may result in drastic changes of the behavior of the material: it may lead to precipitation of polymer aggregates, as found by Joly,[1] to fiber formation,[2-5] or to formation of a second fluid phase.[6,7] A more complete review of the literature is given in Table I, which summarizes published studies of phase separation during mechanical deformation. In addition, we call attention to the excellent reviews of fiber formation in deforming solutions published by McHugh and Forrest[3] and by Peterlin.[4]

A cursory examination of Table I reveals that in many instances mild deformations are sufficient to create phase changes. The formation of aggregates occurs in many flow geometries (cone and plate, concentric cylinders, tube flow, and converging and extensional flows). Its occurrence is quite general for a variety of both polar and nonpolar polymers of high molecular weight in a broad range of concentration (including melts), of temperature, and of solvent type. Dunlop and Cox[30] have additionally considered the importance of aggregate formation in very dilute solutions such as those encountered in turbulent drag reduction.

Several specific examples of the studies cited in Table I illustrate the diversity and permanence of the new phases formed by the deformation of a fluid. Laufer et al.[23] found, using a cone-and-plate viscometer, that polymer particles had precipitated during the shearing process; these re-

† Present address: Instituto de Investigaciones en Materiales, UNAM, Mexico.
‡ Adjunct Professor; Senior Research Associate, Celanese Research Co., Summit, NJ 07901.

0024-9297/84/2217-1187$01.50/0

Table I
Compilation of Literature Data on Stress-Induced Phase Separations in Polymeric Solutions and Melts

polymer–solvent system	crit shear rate, s^{-1}	system used to produce the phenomenon	comments	ref
poly(methacrylic acid) in distilled water	10		irreversible effect	Eliassaf et al.[8]
poly(methyl methacrylate) in dimethyl phthalate	approx 20	cone and plate	small gellike particles	Lodge[9]
polystyrene in dimethyl phthalate	approx 20	cone and plate	small gellike particles	Lodge[9]
muscle proteins in distilled water	100 Hz	oscillatory plate	viscosity changes	Ohnishi[10]
poly(vinyl alcohol) in water	approx 200		irreversible formation of associates	Peter and Noetzel[11]
aqueous solutions of tobacco mosaic virus	approx 14 400	concentric cylinders	irreversible phenomenon	Joly[1]
aqueous solutions of serum albumin	290	concentric cylinders	reversible effect	Joly[1]
poly(methyl methacrylate) in Aroclor	20	cone and plate	reversible phenomenon	Peterlin and Turner[12]
poly(methyl methacrylate) in Aroclor	20	cone and plate	irreversible for large deformations	Peterlin et al.[13]
poly(methyl methacrylate) in Aroclor	20	cone and plate	reversible phenomenon	Peterlin et al.[14]
polyesters and epoxy compounds in toluene and ethylbenzene		concentric cylinders	quasi-crystallites and rheological networks	Steg and Katz[15]
polyethylene in xylene	150 rpm	concentric cylinders, stirrers	irreversibly precipitated	Pennings and Kiel[2]
polyacrylamide Separan AP-30 in distilled water	approx 200	inflow expt	reversible haze	Metzner et al.[6]
polyacrylamide in water		inflow expt	reversible haze	Giesekus[7]
poly(methyl methacrylate) in Aroclor	20	cone and plate	reversible aggregates	Matsuo et al.[16]
polystyrene in Aroclor	approx 150	concentric cylinders	reversible formation	Munk and Peterlin[18]
polystyrene in cyclohexanone	up to 400	concentric cylinders	irreversible	Deveaubois et al.[17]
isotactic polypropylene melt		converging flow	enhanced orientation and melting points	Sieglaff and O'Leary[21]
high-density polyethylene in xylene or diphenyl ether	2000 or more	extensional flow	crystallization	Frank et al.[20]
poly(vinyl alcohol) in distilled water		concentric cylinders	irreversibly precipitated	Yamaura et al.[22]
poly(ethylene oxide) in Aroclor	approx 100	cone and plate	strong time dependence irreversible effect	Laufer et al.[23]
high-density polyethylene melt	50	extensional flow	also observed probable crystallization on flow through screens at 140 °C	Mackley and Keller[24]
polystyrene in DOP	approx 100	capillary and concentric cylinders	reversible phenomenon	Ver Strate and Philippoff[25]
polystyrene in decalin	approx 100	capillary and concentric cylinders	reversible phenomenon	Ver Strate and Philippoff[25]
poly(ethylene oxide) melt		concentric cylinders	obsd an increase in nucleation rate with shearing	Fritsche and Price[26]
polyisobutylene in oil	5	cone and plate		Michele[27]
polyacrylamide dissolved in water–glycerin mixture	order of 10 s^{-1} (exten)	ductless siphon		Kanel[19]
polystyrene in *tert*-butyl acetate		concentric cylinders	reversible	Wolf[28]
polycapramide–caprolactam	1–500	concentric cylinders	reversible and irreversible phenomenon	Malkin et al.[29]

mained undissolved 20 min after cessation of shearing in the case of poly(ethylene oxide) dissolved in a chlorinated biphenyl (Aroclor). Metzner, Cohen, and Rangel-Nafaile[5] and Rangel-Nafaile[31] precipated polyacrylamide from water irreversibly: the 1–5-mm-long fibers formed were insoluble not only in water (normally an excellent solvent) but also in solvents of much higher dissolution power (formamide, morpholine, and glycerin and water containing a mixture of 2 N NaCl and 2 M urea). With glycerin, temperatures as high as 140 °C were employed, and the absence of re-solution was observed for as long as 50 days. At the other extreme, the new phase formed during flow through a large orifice[6,7] or in a Fano (ductless siphon) experiment[19] vanished within seconds after the flow was stopped.

The papers summarized in Table I document the generality of deformation-induced changes in the solubility of polymer solutions and melts. However, only few have attempted any analysis of this phenomenon. The purposes of the present work are to present such an analysis and to compare it with experimental results.

Analysis and Theory

Ver Strate and Philippoff[25] suggested that the stored elastic energy of a flowing polymer solution increased its free energy and thereby changed the phase equilibrium from that of a stagnant solution. They computed the solubility–temperature change by equating the free energy increase resulting from the stored energy to that resulting from phase separation at a higher temperature and found

order-of-magnitude agreement with their experimental observation of changes of the precipitation temperature. They recognized that their analysis was approximate; in fact it would be appropriate only if phase separation into pure components were the process occurring. Their work was important in suggesting the thermodynamic basis for phase separation in flowing solutions and in pointing out the utility of Marrucci's[32] relationship between the solution elasticity and stored free energy to the analysis of the problem.

Wolf[28,33] has also considered the effects of flow upon phase separation of polymer solutions. However, he treats a different physical problem, namely the equilibrium size of the droplets which are formed when phase separation occurs as determined by the combined effects of shear and normal stresses and of interfacial tension. He proposes that the equilibrium droplet size is decreased by shearing and that when it approaches the radius of gyration of the polymer molecules, re-dissolution will have occurred. Wolf's model predicts that the solubility temperature is decreased by flow, in contrast to the Ver Strate and Philippoff observation and calculation that it is increased.

However, there is not necessarily a contradiction between these two results because, as stated above, the two investigators are describing different phenomena, which may occur under different experimental conditions. In fact, Wolf[33] finds with the system studied by Ver Strate and Philippoff (polystyrene in dioctyl phthalate) that the initial turbidity occurs at a higher temperature in a stirred solution than in a stagnant one. It is only at still lower temperatures that the turbidity curves cross. Wolf does not interpret his results as confirming those of Ver Strate and Philippoff, but his reasons are not clear to the present authors.

In the present work we shall take the free energy of mixing n_1 moles of solvent with n_2 moles of polymer to be given (for stagnant solutions) by the Flory–Huggins equation:[34,35]

$$\Delta G_M = RT[n_1 \ln (1 - \phi) + n_2 \ln \phi + \chi_1\phi(1 - \phi)N] \quad (1)$$

where R is the gas constant, T is the absolute temperature, ϕ is the volume fraction of polymer, and N is given by $N = n_1 + mn_2$, with m the molar volume of polymer divided by the molar volume of solvent; χ_1 is the interaction parameter. In the present treatment χ is assumed to be a constant, independent of concentration. It is known that χ may in fact depend upon concentration,[34] but, as shown experimentally below, for the relatively narrow range of concentrations studied in this work, the assumption of a constant χ is adequate for representation of the data. The change in the free energy of mixing upon imposing a steady-state deformation process may be calculated from the trace of the deviatoric stress tensor $\mathbf{P}$, which is a measure of the molecular deformation, as[32]

$$\Delta G^s = \tfrac{1}{2} \text{ tr } \mathbf{P} \quad (2)$$

For the elastic dumbbell model of molecular conformation, upon which eq 2 is based, tr $\mathbf{P}$ is also equivalent to the first normal stress difference if we have a steady laminar shearing flow, and so this increment ΔG^s in the free energy change is readily accessible experimentally. Thus the free energy of mixing of stagnant polymer and solvent to form a flowing solution is then obtained simply as

$$\Delta G_M^* = RT[n_1 \ln (1 - \phi) + n_2 \ln \phi + \chi_1\phi(1 - \phi)N] + \frac{\upsilon N}{2} \text{ tr } \mathbf{P} \quad (3)$$

Some comments may be made about this expression. The theoretical basis for the thermodynamics of elastic fluids in a steady state under the influence of an external field, rather than at static equilibrium, was developed by Coleman.[53] Discussions of this approach are available, for example by Truesdell[54] and, particularly accessibly, by Astarita and Marrucci.[55] The particular form of the stored elastic energy that is used was derived by Marrucci[32] for a dilute solution of elastic dumbbells. However, Marrucci points out that the result of his calculation may be applicable to a broader range of materials, just as the constitutive equation corresponding to the dumbbell model is. The identity of form of the constitutive equations for the dilute dumbbells and for an entanglement network model[56] is one example perhaps of the applicability of such equations beyond the exact conditions for which they were derived. Another analogy may be drawn between Marrucci's result for the stored energy of a dumbbell solution with the identical result, at large deformations, for an ideal rubber.[57]

The additivity of the free energies in eq 3 is an additional assumption. It implies that free energy of mixing (eq 1) is not affected by the polymer coil deformation responsible for the stored elastic energy (eq 2).

In order to apply eq 3, an expression for χ_1 is necessary. This is given[34] as

$$\chi_1 = \tfrac{1}{2} + \Psi_1[(\Theta/T) - 1] \quad (4)$$

When a homogeneous solution is cooled so that it separates into two phases which are in thermodynamic equilibrium with each other, the conditions for equilibrium may be shown to be[34]

$$\mu_1^{\text{I}} = \mu_1^{\text{II}}$$
$$\mu_2^{\text{I}} = \mu_2^{\text{II}} \quad (5)$$

The chemical potentials μ_i are, in the form most suitable for computation from experimental data,

$$\mu_1 = \overline{\Delta G_M} - x_2\left[\frac{\partial(\overline{\Delta G_M})}{\partial x_2}\right]_{T,P,x_1} \quad (6)$$

$$\mu_2 = \overline{\Delta G_M} + x_1\left[\frac{\partial(\overline{\Delta G_M})}{\partial x_2}\right]_{T,P,x_1} \quad (7)$$

Here, the $\overline{\Delta G_M}$ denote the change in free energy on forming the solution from the reference state of pure polymer and pure solvent. Equations 6 and 7 require the partial differentiation of the molar free energy of mixing (in this particular case ΔG_M has been replaced by $\overline{\Delta G_M}$, where $\overline{\Delta G_M} = (\Delta G_M)/(n_1 + n_2)$).

By analogy to the analysis for stagnant solutions,[35] the chemical potentials of deforming fluids may be calculated from eq 3, 6, and 7, but modified to account for the state of deformation of the solution.

For a stagnant solution the parameters that remain constant during the differentiation are T, P, and x_1, as stated in eq 6 and 7. In the case treated here, where there is a mechanically induced deformation of the solution, one additional parameter is needed for the description of the physics of phase separation: it is the state of stress under which the process takes place. If the droplets of the new phase being formed are not too small and do not possess surface rigidity, then the surface shearing and normal stresses will both be continuous across the interface.[36] This is the assumption used in the present work. The corresponding expressions for the chemical potentials are then

$$\mu_1^* = \overline{\Delta G_M}^* - x_2\left(\frac{\partial}{\partial x_2}\overline{\Delta G_M}^*\right)_{T,P,x_1,P_{12}} \quad (8)$$

$$\mu_2^* = \overline{\Delta G_M}^* + x_1\left(\frac{\partial(\overline{\Delta G_M}^*)}{\partial x_2}\right)_{T,P,x_1,P_{12}} \quad (9)$$

Here, P denotes the isotropic pressure to which the system is subjected and P_{12} denotes the shearing stress being applied to the deforming system.

The equilibrium concentrations will be computed as usual by determining the concentration at which the chemical potentials of both components are equal in the two phases in equilibrium. The evaluation, as discussed below, was by numerical methods. An approximate analytical treatment is given in the appendix; it serves to confirm the numerical results and also provides some insight into the nature of the equilibrium.

Experimental Section

The system studied was high molecular weight polystyrene (PS) dissolved in dioctyl phthalate (DOP). The polymer was manufactured by Pressure Chemical Co. and had a molecular weight $M_w = 1.8 \times 10^6$, with a polydispersity (M_w/M_n) of 1.3. The solvent was manufactured by Alfa Products. It has a molecular weight 390.6 and density 0.9 g/cm^3. The concentrations of the solutions in grams of polymer per milliliter of solution were 0.0195, 0.0421, 0.0572 and 0.0776. Solutions were prepared by gentle agitation of weighed quantities of polymer and solvent at 60 °C.

These different sets of experiments were carried out in order to obtain the information required. First, the interaction parameter χ_1 had to be determined experimentally for the system PS in DOP, by measurement of the solubility curves of stagnant solutions. Second, shearing and normal stresses (rheological properties) had to be measured, the former as a function of temperature. Finally, flow-induced phase separation was observed by using two flow geometries: torsional flow in a cone-and-plate geometry and Poiseuille flow through a tube.

(a) Interaction Parameter Measurement. The interaction parameter χ_1 was determined by determining the phase diagram of the PS–DOP system with three samples of PS of different molecular weights. Solubility curves of solutions of various concentrations of each polymer were observed from both the appearance of cloudiness upon slow cooling and its disappearance upon warming; details of the experimental procedure are given elsewhere.[31] The reciprocals of the upper critical solution temperatures were plotted against the reciprocal of the square root of the molar volume ratio[34] in the usual way. The intercept is the reciprocal of the theta temperature, Θ, and the slope is $(\Psi\Theta)^{-1}$. With these data it is then possible to calculate the temperature dependent interaction parameter χ_1 as

$$\chi_1 = \frac{1}{2} + \Psi_1\left(\frac{\Theta}{T} - 1\right) \quad (10)$$

The results were $\Theta = 288 \pm 0.5$ K and $\Psi_1 = 1.48 \pm 0.09$. The experimental results and the solubility curves calculated with the parameters are shown in Figure 1. For comparison, previously reported results for Θ are 285 and 295 K, as determined by viscosity[37] and by light scattering[38] methods. While the relatively narrow molecular weight range used and the polydispersity of one of the samples used limit the accuracy of the values reported here, we should note that we are primarily interested in deviations from the uppermost stagnant solubility curve of Figure 1, which is seen to be fitted well by the values cited.

(b) Rheological Data. Measurements of the shearing stress P_{12}, as a function of deformation rate and polymer concentration, were made at temperatures of 15, 25, and 35 °C. From these data and the time–temperature superposition principle,[39,40] the temperature shift factors could be evaluated for all solutions. As shown previously for a similar fluid (polystyrene in toluene) by Kotaka, Kurata, and Tamura[41] these shift factors are expected to be applied equally to the normal stress data; consequently this quantity was obtained only at 25 °C but for all four concentration levels of interest. In order to verify the applicability of the temperature shift factor to the normal stress measurements, linear viscoelastic data were also taken at all three temperatures. In fact, however, their accuracy was sufficiently limited to render them of relatively little value since the fluids were not highly elastic at the higher temperature levels. They did not, however, contradict the above choice of temperature dependency. In passing, we should also note that the superposition of linear and steady-state rheological measurements for dilute solutions in viscous solvents cannot be carried out in the conventional manner.[42]

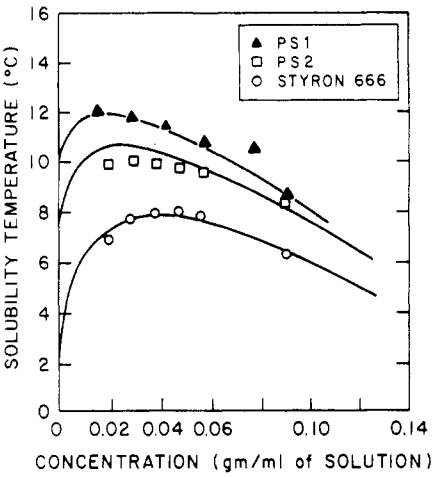

Figure 1. Solubility diagram for three different samples of polystyrene in dioctyl phthalate. Points represent actual data; solid lines indicate theoretical predictions of eq 10. Styron 666 is a commercial product with a broad molecular weight distribution. The uppermost curve (PS1) is for the polymer used later in studies of deformational effects and has an M_w of 1.8×10^6; the middle curve is for a lower M_w of 9×10^5.

(c) Cloud Point Determinations in Deforming Solutions. In order to show that effects of deformation upon solubility were independent of the choice of a particular mode of shearing or apparatus geometry, two sets of data were taken using, for the first, laminar Poiseuille flow through a tube and, for the second, torsional flow in a cone-and-plate geometry.

Poiseuille flow experiments were carried out with a pair of slightly tapered glass tubes immersed in a thermostated transparent reservoir. The fluid was pushed through one of the capillary tubes by a nitrogen-pressurized reservoir; the other capillary tube, filled with the same but stagnant fluid, served as a reference sample. By varying the flow rate slowly, the onset of visible cloudiness of each solution at a given temperature was determined at a specific point of the slightly tapered section of the tube. The clouding of the solution was reversible, turbidity fading in about 1 s after the flow was stopped.

Cone-and-plate observations of the cloud point as a function of temperature and deformation rate were carried out in a rheogoniometer fitted with a transparent plastic cone and plate as described by King and Copley.[43] Temperature-controlled water was circulated through the hollow plate; its temperature was continually monitored with a thermistor, and frequent spot checks of the actual temperature of the test fluid itself were made by inserting a second thermistor probe into the shearing fluid. These showed the two temperatures to be identical within experimental error. The cone used in our work had a diameter of 5 cm and a cone angle of 1°. The shear rate was progressively increased, in 1.6-fold steps, from its lowest value until cloudiness of the solution was visually apparent. The range of shear rates covered was from 1.7 to 1360 s^{-1}. A fresh sample of solution was charged for each temperature.

The fact that shear rates cannot be varied continuously in the rheogoniometer used, as in the case of the Poiseuille flow experiments, means that only a range of shear rates may be cited within which the cloudiness of the solution first occurred, rather than a point value, and it is this range which will be compared with the data from the Poiseuille flow experiments. While the absence of point values may be a disappointment for precise work, it is a decided advantage in scouting experiments as the solution cloudiness becomes so intense, when the shear rate is stepped up to its next higher value, that little ambiguity exists concerning

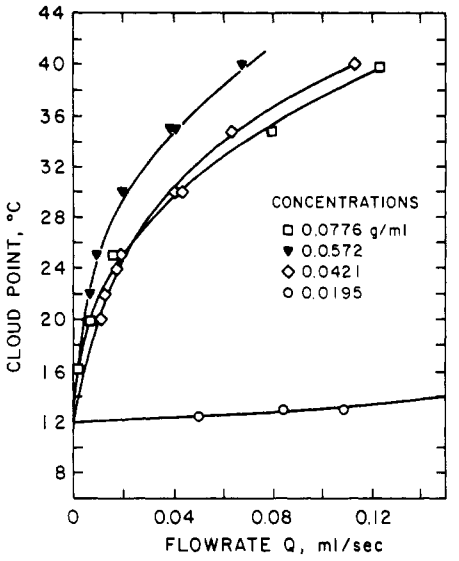

Figure 2. Plot of the cloud point as a function of flow rate for solutions of high molecular weight polystyrene (PS1).

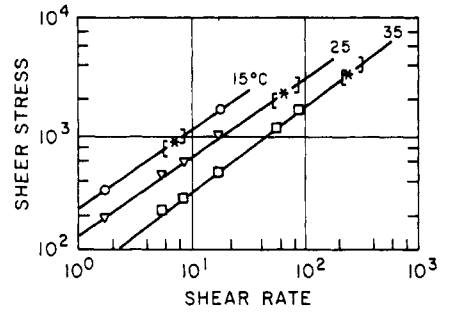

Figure 3. Shear stress–shear rate data for PS1 solutions at a concentration level of 0.0421 g/mL. The regular data points denote experimental stress measurements in the cone-and-plate geometry. The brackets on each curve depict the shear rate intervals within which cloudiness first appeared in the (transparent) cone-and-plate apparatus and the asterisks denote the shear rate at which cloudiness was first detected in the Poiseuille experiment using transparent capillary tubes. Stresses are given dyn/cm^2; shear rates in s^{-1}.

the ability to recognize an incipient phase change.

The shearing stresses were also recorded as a function of time, and the solution was observed visually to detect the occurrence of turbidity. It was found that the onset of cloudiness coincided with a change in the transient shear stress: when the solutions remained transparent, the stress reached and maintained a constant value very quickly after the shearing was begun. Contrarily, at shear rate levels leading to cloudiness (phase change) the stress exhibited a large overshoot, which was then followed by a period of irregular behavior and slow stress decay before finally reaching a steady value. Thus incipient changes in solution clarity, frequently difficult to observe visually, could be readily verified by the comparatively dramatic changes in the stress tracing, which have been carefully documented in the dissertation.[31] Similar observations of the behavior of the transient shearing stress, when phase changes occur, have been reported by Munk and Peterlin,[18] Laufer et al.,[23] and Michele.[27]

Measurements of the shear rate, and of the stress, at the solution cloud point, were made at 15, 25, and 35 °C in the cone-and-plate geometry and at 12, 15, 20, 22, 25, 30, 35, and 40 °C in the Poiseuille flow experiment. Solution concentrations of 0.0421, 0.0572, and 0.0776 g/mL of polymer were used in both experiments. Additionally, some data were obtained at 0.0195 g/mL for the Poiseuille experiment alone.

Results and Comparison with Theory

Figure 2 shows the results of the capillary tube experiments at the four concentrations of polymer. At the lowest concentration, 0.02 g/mL, there are measurable but

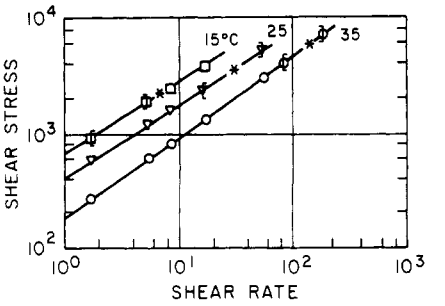

Figure 4. Data as in Figure 3 but concentration level of polymer is 0.0572 g/mL.

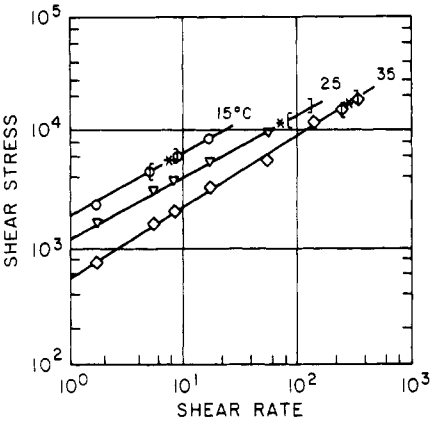

Figure 5. As Figure 3 for concentration level of 0.0776 g/mL.

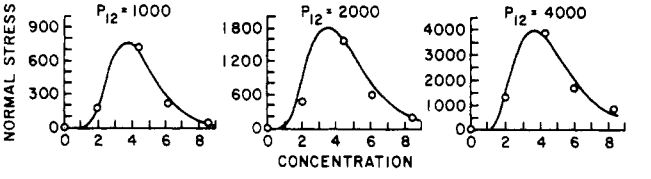

Figure 6. Plots of normal stress, or trace of the stress tensor, as a function of concentration, at 35 °C, for three different shearing stress levels. All stresses given in units of dyn/cm^2.

only minor changes in cloud point with deformation state of the system. However, at the 0.06 g/mL concentration level, changes as great as 28 °C were recorded at a flow rate of only 0.066 mL/s. The diameter of the transparent tube at the point of measurement was 0.146 cm, giving a wall shear rate computed as $32Q/\pi D^3$ of only 220 s^{-1} at this flow rate. We believe that a 28 °C change in cloud point accompanying such a small deformation rate change is a dramatic manifestation of the large changes in polymer solubility which may be induced by shearing the solution, i.e. of the importance of the Marrucci term in eq 3. The reasons for the nonmonotonic changes of the curves with concentration level, in Figure 2, will become clear shortly (no pun intended).

Figures 3–5 compare, using shear stress–shear rate plots, the conditions of onset of opacity as observed in the two independent experiments. One sees excellent agreement.

In order to compute the solubility curves under shear the differentiations indicated in eq 8 and 9 were carried out numerically. The procedure was quite tedious; it is described in detail elsewhere[31] and is only summarized here.

Having estimated the normal stress, or tr **P** (in eq 3), as a function of temperature, it is possible to cross-plot the data in order to express the normal stress as a function of concentration at constant shearing stress and temperature—as required for evaluation of the derivatives in eq 8 and 9. Typical plots of this dependence are shown in Figure 6. In order to perform the numerical differen-

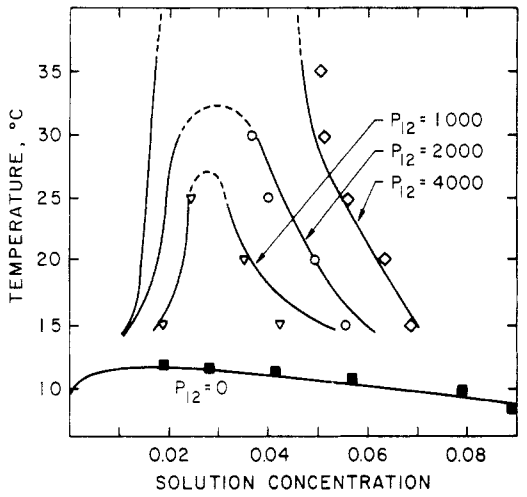

Figure 7. Solubility diagram for stagnant and deforming solutions: comparison of theory and experiment. Solution concentrations expressed in g/mL.

tiation, the points in Figure 6 were fitted to an empirical interpolation equation, shown as a solid line in each case of Figure 6.

The reasons for the maxima in these curves are straightforward: at zero concentration, the normal forces are, of course, zero, as the fluid is Newtonian. Addition of polymer increases the normal force progressively and the curve rises. As higher concentrations are reached, however, the shear rate at which the experimental measurements are made progressively decreases (since the fluid viscosity increases with concentration and, in Figure 6, the shearing stress is held constant in a given figure). Consequently, as very high concentrations are reached, the deformation rate, and hence the normal forces, again goes to zero. These same arguments serve to explain the irregular concentration–cloud point trends observed earlier in Figure 2.

The empirical curves shown in Figure 6, and the measurements of the solubility parameter χ_1, enable calculation of ΔG_M^* (eq 3) at any desired shear stress and temperature level. The numerical differentiation of ΔG_M^* in eq 8 and 9 was performed by using the Lagrangian interpolation polynomial of degree two fitted to three neighboring and successive points.[44] In this way calculations of the activity coefficients μ_1^* and μ_2^* were made at three shear stresses at each of five temperatures and at numerous concentrations using very small increments of concentration in the region of interest. It was thereby possible to identify graphically, at each stress and temperature, the two concentrations at which the chemical potentials of both components were equal, as required for equilibrium. The Fortran program and sample printouts are available.[31]

The computed solubility or cloud-point curves are shown in Figure 7 for four levels of the shearing stress (0, 1000, 2000 and 4000 dyn/cm^2) for PS1 in dioctyl phthalate. Also depicted as individual points are the experimental results as interpolated, at the arbitrary stress levels chosen, from the data for Figure 2 and the rheological measurements (Figures 3–5). Qualitatively, the agreement between theory and experiment appears to be reasonable.

In order to compare all of the measurements directly and quantitatively with the theoretical predictions, at the actual stress, deformation rate, and temperature levels of the individual experiments, Figure 8 was prepared. In doing so, three data points for the most concentrated solution were eliminated because these required major extrapolations of the measured rheological parameters. The mean deviation of all the remaining data taken under conditions

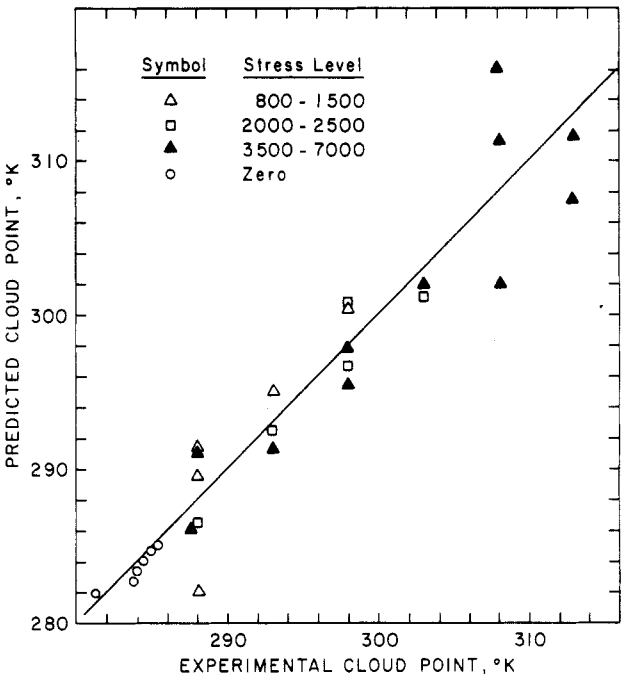

Figure 8. Comparison of theory and experiment: calculated cloud points compared to experimental observations. Shearing stress levels given in dyn/cm^2.

of finite stress level, from the 45° line depicting perfect agreement, was 2.8 K. It is worth noting that although the treatment of the data required considerable manipulation (curve fitting and differentiation of data and use of the time–temperature superposition principle), no adjustable parameters of any kind were employed.

Discussion and Concluding Remarks

The solubility temperature (cloud point) of a polymer solution is a function of the shear rate to which the solution is subjected. Changes of as much as 28 °C from the stagnant solution precipitation temperature have been observed. The solubility curves of sheared solutions can be predicted satisfactorily (Figure 8) from thermodynamic parameters derived from measurements on stagnant solutions by considering that the free energy of the solution is additive with the stored elastic energy as estimated by the trace of the stress tensor.

There are obvious implications of this result for processes in which polymeric fluids are subjected to high deformation rates. Confirmation and extension of the present results are therefore desirable. Of interest are the effects of molecular weight, of polydispersity, of polar and ionic interactions, and of polymer–solvent interaction parameter. Also, it would be interesting, although perhaps more difficult, to observe the effect with kinematics other than simple shear: in view of the enormously greater stress levels imposed upon the molecules during extensional flows,[20,45–51] especially in solutions, such deformation fields may be of especial interest both theoretically and pragmatically.

In conclusion, the qualitative results reviewed in Table I make it abundantly clear that the deformation state of polymeric melts and solutions is as important a primary state variable, in a thermodynamic sense, as are the more familiar state variables of temperature, pressure, and composition. The present contribution shows how the effect of deformation state on system free energy appears to be quantitatively accessible through easily measured rheological properties. Sufficient unresolved questions remain to make this area a fertile one for further theoretical and experimental studies.

Acknowledgment. R. B. King carried out the careful rheogoniometric measurements using his transparent cone-and-plate assembly. A. Villanueva assisted in the numerical computations; S. J. Lee and R. K. Gupta contributed in innumerable discussions. Financial support was provided by grants from Exxon Production Research Co. and the Exxon Education Foundation and by CONACYT (Consejo Nacional de Ciencia y Tecnologia) and UNAM through the Programa de Superacion del Personal Academico.

Appendix A

In order to check independently the numerical results from the computer program, for computation of phase equilibria, and to gain whatever insights are afforded by an analytical solution to the equations for phase equilibrium, it was attempted to find such a solution.

It is possible to find a simple solution for the critical point. The equation can be solved exactly if, in the neighborhood of the critical point, the dependence of the normal stress upon concentration (at constant shear stress and temperature) can be expressed as a quadratic. This derivation is described first.

Somewhat more lengthy, but still straightforward, is the answer to the question: How is the quiescent phase equilibrium perturbed by the stored elastic energy, in the limit of small (first-order differentials) changes of the concentration and interaction parameter by the stress? The solution to this problem with quadratic dependence of normal stress upon concentration gives exactly the same answer as the above solution for the change in the critical point. The derivation of this solution is described next.

Third, the numerical predictions of this analytical solution are compared with the numerical results presented in the body of the paper and are shown to be in remarkable agreement.

Finally, some interesting conclusions that suggest directions for further work are drawn from consideration of the analytical solution.

Effect of Stress upon the Critical Point. The starting point of the analysis is the expression (A-1) for the free energy of mixing ΔG of the stressed solution, assuming that the stored elastic energy is additive to the ordinary free energy, which is taken to be the Flory–Huggins equation

$$\frac{\Delta G_M^*}{RT} = n_1 \ln (1-\phi) + n_2 \ln \phi + \chi_1 \phi(1-\phi)N + \frac{\upsilon N \text{ tr } \mathbf{P}}{2RT} \quad \text{(A-1)}$$

where n_1 is the moles of solvent, n_2 is the moles of polymer, m is the molar volume of polymer/molar volume of solvent, χ_1 is the interaction parameter, ϕ is the volume fraction of polymer, tr $\mathbf{P}$ is the trace of the stress tensor, υ is the molar volume of solvent, $N = n_1 + mn_2$, and $\phi = mn_2/N$. The chemical potentials μ_i are as usual

$$\mu_i = \partial \Delta G_M^* / \partial n_i$$

Carrying out the differentiation for the solvent (and factoring out RT for convenience and denoting this reduced chemical potential by μ_i^*)

$$\mu_1^* \equiv \frac{\mu_1}{RT} = \ln (1-\phi) + \left(1 - \frac{1}{m}\right)\phi + \chi\phi^2 + \frac{\upsilon}{2RT}\left[\text{tr } \mathbf{P} - \phi \frac{\partial \text{ tr } \mathbf{P}}{\partial \phi}\right] \quad \text{(A-2)}$$

The conditions for the critical point are[35]

$$\frac{\partial \mu_1^*}{\partial \phi} = \frac{1}{RT}\frac{\partial \mu_1}{\partial \phi} = 0$$

$$\frac{\partial^2 \mu_1^*}{\partial \phi^2} = \frac{1}{RT}\frac{\partial^2 \mu_1}{\partial \phi^2} = 0 \quad \text{(A-3)}$$

Again carrying out the differentiations, the results are

$$-\frac{1}{1-\phi} + \left(1 - \frac{1}{m}\right) + 2\phi\chi - \frac{\upsilon}{2RT}\phi \frac{\partial^2 \text{ tr } \mathbf{P}}{\partial \phi^2} = 0 \quad \text{(A-4)}$$

and

$$-\frac{1}{(1-\phi)^2} + 2\chi - \frac{\upsilon}{2RT}\left[\frac{\partial^2 \text{ tr } \mathbf{P}}{\partial \phi^2} + \phi \frac{\partial^3 \text{ tr } \mathbf{P}}{\partial \phi^3}\right] = 0 \quad \text{(A-5)}$$

Now, it is assumed that near the maximum in the curves of Figure 6 the experimental data can be approximated adequately by a parabola:

$$\text{tr } \mathbf{P}(\phi) = a(\phi - \phi_m)^2 + b\phi + \text{tr } \mathbf{P}_m \quad \text{(A-6)}$$

from which

$$\partial \text{ tr } \mathbf{P}/\partial \phi = 2a(\phi - \phi_m) + b$$

$$\partial^2 \text{ tr } \mathbf{P}/\partial \phi^2 = 2a \quad \text{(A-7)}$$

$$\partial^3 \text{ tr } \mathbf{P}/\partial \phi^3 = 0$$

Substitution of these derivations into (A-4) and (A-5) gives

$$-\frac{1}{1-\phi} + \left(1 - \frac{1}{m}\right) + 2\phi\chi - \frac{a\upsilon}{RT}\phi = 0 \quad \text{(A-4}^1\text{)}$$

and

$$-\frac{1}{(1-\phi)^2} + 2\chi - \frac{a\upsilon}{RT} = 0 \quad \text{(A-5}^1\text{)}$$

The analogous equations for the quiescent solution are[35]

$$-\frac{1}{1-\phi} + \left(1 - \frac{1}{m}\right) + 2\phi\chi^\circ = 0 \quad \text{(A-8)}$$

and

$$-\frac{1}{(1-\phi)^2} + 2\chi^\circ = 0 \quad \text{(A-9)}$$

Equations A-8 and A-9 have the well-known solutions

$$\phi_c = 1/(1 + m^{1/2}) \quad \text{(A-10)}$$

$$\chi_c^\circ = \tfrac{1}{2}(1 + m^{-1/2})^2 \quad \text{(A-11)}$$

The most simple way to solve eq A-4^1 and A-5^1 is to make the substitution

$$\chi = \chi^\circ + a\upsilon/2RT \quad \text{(A-12)}$$

which identically reduces (A-4^1) and (A-5^1) to (A-10) and (A-11). Equation A-12 is therefore the derived solution. In other words, the concentration at the critical point is not changed (to within the approximation (A-6)) by stress, but the interaction parameter is shifted by the amount

$$\Delta\chi = a\upsilon/2RT \quad \text{(A-13)}$$

Effect of Stress upon Binodal. The conditions that determine the phase equilibrium or binodal are

$$\mu_1(\phi) = \mu_1(\phi')$$

$$\mu_2(\phi) = \mu_2(\phi') \quad \text{(A-14)}$$

at two concentrations ϕ and ϕ'. We now ask: If we know

the binodal for the quiescent solution, can we calculate how this is perturbed by the normal stress term in eq A-1? If we denote the values for the quiescent solutions by μ_1° and μ_2°, then carrying out the required differentiations of (A-1) we obtain

$$\mu_1^* \equiv \frac{\mu_1}{RT} = \frac{\mu_1^\circ}{RT} + \frac{v}{2RT}\left[\text{tr } \mathbf{P} - \phi\frac{\partial \text{ tr } \mathbf{P}}{\partial\phi}\right] \quad \text{(A-15)}$$

$$\mu_2^* \equiv \frac{\mu_2}{RT} = \frac{\mu_2^\circ}{RT} + \frac{mv}{2RT}\left[\text{tr } \mathbf{P} + (1-\phi)\frac{\partial \text{ tr } \mathbf{P}}{\partial\phi}\right] \quad \text{(A-16)}$$

The method used to determine the perturbation of the quiescent binodal curve is perhaps best carried out by visualizing a graphical construction on a plot of solubility parameter vs. volume fraction of polymer, ϕ. Consider first a curve that satisfies condition (A-14) in the absence of stress. Select arbitrarily two concentrations ϕ and ϕ_a on this curve that are in equilibrium, i.e. correspond to the same value of χ, say χ°.

Now, assume that the effect of the elastic energy is to shift the interaction parameter of the solution of concentration ϕ to some new value $\chi^\circ + \Delta\chi$. The concentration in equilibrium with ϕ is now no longer necessarily ϕ_a but may be shifted by some amount $\Delta\phi_a$ to $\phi_a + \Delta\phi_a$. Finding $\Delta\chi$ and $\Delta\phi_a$ will determine a point on the new binodal in the presence of stress.

The chemical potentials of the solvent and of the polymer are now expanded about their quiescent equilibrium values

$$\mu_1(\phi + \Delta\phi, \chi + \Delta\chi) = \mu_1^\circ(\phi, \chi) + \frac{\partial\mu_1^\circ}{\partial\chi}\Delta\chi + \frac{\partial\mu_1^\circ}{\partial\phi}\Delta\phi + \frac{v}{2RT}\left[\text{tr } \mathbf{P} - \phi\frac{\partial \text{ tr } \mathbf{P}}{\partial\phi}\right] \quad \text{(A-17)}$$

$$\mu_2(\phi + \Delta\phi, \chi + \Delta\chi) = \mu_2^\circ(\phi, \chi) + \frac{\partial\mu_2^\circ}{\partial\chi}\Delta\chi + \frac{\partial\mu_2^\circ}{\partial\phi}\Delta\phi + \frac{mv}{2RT}\left[\text{tr } \mathbf{P} + (1-\phi)\frac{\partial \text{ tr } \mathbf{P}}{\partial\phi}\right] \quad \text{(A-18)}$$

The partial derivatives required are

$$\partial\mu_1^\circ/\partial\chi = \phi^2$$

$$\partial\mu_1^\circ/\partial\phi = -[1/(1-\phi)] + (1 - 1/m) + 2\phi\chi$$

$$\partial\mu_2^\circ/\partial\chi = m(1-\phi)^2$$

$$\partial\mu_2^\circ/\partial\phi = 1/\phi + (m-1) - 2m(1-\phi)\chi \quad \text{(A-19)}$$

Also, for convenience of manipulation we define the auxiliary variables

$$Y(\phi) \equiv \frac{v}{2RT}\left[\text{tr } \mathbf{P}(\phi) - \phi\left.\frac{\partial \text{ tr } \mathbf{P}}{\partial\phi}\right|_\phi\right]$$

$$Z(\phi) \equiv \frac{mv}{2RT}\left[\text{tr } \mathbf{P}(\phi) + (1-\phi)\left.\frac{\partial \text{ tr } \mathbf{P}}{\partial\phi}\right|_\phi\right] \quad \text{(A-20)}$$

We are now ready to write out explicitly the quantities in the equilibrium conditions (A-14) for the points of composition ϕ and ϕ_a. For the solvent

$$\mu_1(\phi_a + \Delta\phi_a, \chi + \Delta\chi) = \mu_1(\phi, \chi + \Delta\chi)$$

$$\mu_1(\phi_a + \Delta\phi_a, \chi + \Delta\chi) = \mu_1^\circ(\phi_a) + Y(\phi_a) + (\phi_a)^2\Delta\chi + \left[\left(-\frac{1}{1-\phi_a}\right) + \left(1 - \frac{1}{m}\right) + 2\phi_a\chi\right]\Delta\phi_a$$

$$\mu_1(\phi, \chi + \Delta\chi) = \mu_1^\circ(\phi) + Y(\phi) + \phi^2\Delta\chi$$

Remembering that $\mu_1^\circ(\phi_a) = \mu_1^\circ(\phi)$, these lead to

$$Y(\phi) - Y(\phi_a) + (\phi^2 - (\phi_a)^2)\Delta\chi = C\Delta\phi_a \quad \text{(A-21)}$$

where again for convenience we define C by

$$C \equiv \left(-\frac{1}{1-\phi_a}\right) + \left(1 - \frac{1}{m}\right) + 2\phi_a\chi \quad \text{(A-22)}$$

Carrying out the analogous procedure for μ_2

$$[Z(\phi) - Z(\phi_a)] + m[(1-\phi)^2 + (1-\phi_a)^2]\Delta\chi = F\Delta\phi_a \quad \text{(A-23)}$$

where F is defined by

$$F \equiv 1/\phi_a + (m-1) - 2m\chi(1-\phi_a) \quad \text{(A-24)}$$

Equations A-21 and A-23 are simultaneous linear algebraic equations in the two unknowns $\Delta\chi$ and $\Delta\phi_a$ and are of the form

$$A + B\Delta\chi = C\Delta\phi_a$$

$$D + E\Delta\chi = F\Delta\phi_a \quad \text{(A-25)}$$

where the coefficients $A, B, \ldots, F$ are known constants for any pair of concentrations in equilibrium on the known quiescent phase diagram. (A-25) can therefore be solved to give

$$\Delta\chi = -\frac{(1-\phi_a)mA + \phi_a D}{m(\phi - \phi_a)^2}$$

and

$$\Delta\phi_a = (A + B\Delta\chi)/C \quad \text{(A-26)}$$

However, to evaluate these expressions it is necessary to assume a functional form for tr $\mathbf{P}(\phi)$, since tr $\mathbf{P}$ and ∂ tr $\mathbf{P}/\partial\phi$ occur in the coefficients A and D.

Assuming again the form (A-6), after some tedious but straightforward algebra, the astonishingly simple result is obtained

$$\Delta\phi_a = 0$$

$$\Delta\chi = av/2RT \quad \text{(A-27)}$$

We note first that this result is precisely the one derived in a much simpler fashion in the previous section for the critical point. This provides a check on the correctness of the algebra of the present procedure. The result (A-27) means that, to within the approximations of small perturbation and of the quadratic dependence of tr $\mathbf{P}$, the effect of stress is merely to shift the spinodal parallel to the quiescent spinodal along the χ axis.

Numerical Evaluation and Comparison with Computer Results. Using eq 10

$$\chi = \frac{1}{2} - \Psi\left(1 - \frac{\Theta}{T}\right)$$

we obtain

$$\Delta T = -\frac{T^2}{\Psi\Theta}\Delta\chi \quad \text{(A-28)}$$

Using $v = 390$ cm^3/mol, $T \sim 300$ K, $\Theta = 288$ K, $\Psi = 1.48$, eq A-28 and A-27 result in

$$\Delta T \approx -1.5 \times 10^{-6}a \quad \text{(A-29)}$$

where, it is recalled, a is the coefficient of the quadratic

term in eq A-6. Fitting the normal stress data we obtain the following results:

	P_{12}, dyn/cm²		
	1000	2000	4000
a	-1.15×10^6	-2.9×10^6	-7.0×10^6
ΔT(calcd), deg	1.7	4.4	10.5
ΔT(measd)	4	14	24

Two questions come to mind in considering the agreement between the numerical procedure in the text and the approximate analytic treatment of this appendix. First, do the results agree reasonably well in magnitude? The comparison in the table above indicates that the two procedures agree to within a factor of 2–3. This agreement is satisfactory if one considers that the calculated ΔT is proportional to the second derivative of the normal stress vs. concentration curve and that only a simple quadratic function was used to depict this. Second, the prediction of the analytic solution is that the shape of the spinodal is unchanged by stress and only shifted along the χ or T axis. This is not apparently the situation depicted in Figure 7. One may again appeal to the sensitivity of the prediction to very small errors in the original data to account for the apparent difference between the two methods of calculation, since the differentiation of normal stress data is, at best, a very difficult procedure. Further, the temperature changes shown in Figure 7 do not represent first-order differential changes.

Further Considerations from the Analytic Results. It is worth noting once more the effect of the shape of the tr **P** vs. ϕ curves of Figure 6. For entangled polymer solutions this dependence is generally[52] given as

$$\text{tr } \mathbf{P} \approx 2J_e P_{12}^2$$

with $J_e \sim \phi^{-1}$ or ϕ^{-2}. Therefore, at constant shear stress P_{12}, as assumed, tr **P** will be proportional to ϕ^{-1} or ϕ^{-2}. But with this dependence the second derivative (a in eq A-6) is positive; e.g., the tr **P** vs. ϕ curve is concave upward. The prediction is therefore that the spinodal would be shifted to lower temperatures rather than higher as found experimentally.

In fact, the experimental tr **P** vs. ϕ curves go through a maximum, i.e. are concave downward, and the theory therefore does predict the correct dependence of cloud point temperature on stress. This may be related to the fact that for the present solutions the maxima in Figure 6 are close to the critical entanglement concentrations[52] of the system, and other polymer solutions or different molecular weight levels of the polymer may lead to appreciably different results, including, for lower molecular weight polymers, no measurable change in the cloud point with deformation rate level.

Registry No. Polystyrene (homopolymer), 9003-53-6.

References and Notes

(1) M. Joly, *Kolloid Z.*, **182**, 133 (1962).
(2) A. J. Pennings and A. M. Kiel, *Kolloid Z. Z. Polym.*, **205**, 160 (1965).
(3) A. J. McHugh and E. H. Forrest, *J. Macromol. Sci., Phys.*, **B11** (2), 219 (1975).
(4) A. Peterlin, *Polym. Eng. Sci.*, **16**, 126 (1976).
(5) A. B. Metzner, Y. Cohen, and C. Rangel-Nafaile, *J. Non-Newtonian Fluid Mech.*, **5**, 449 (1979).
(6) A. B. Metzner, E. A. Uebler, and C. F. Chan Man Fong, *AIChE J.*, **15**, 750 (1969).
(7) H. Giesekus, *Rheol. Acta*, **8**, 411 (1969).
(8) J. Eliassef, A. Silverberg, and A. Katchalsky, *Nature (London)*, **176**, 1119 (1955).
(9) A. S. Lodge, *Polymer*, **2**, 195 (1961).
(10) T. Ohnishi, *J. Polym. Sci.*, **62**, S42 (1962).
(11) S. Peter and W. Noetzel, *Kolloid Z.*, **183**, 97 (1962).
(12) A. Peterlin and D. T. Turner, *J. Polym. Sci., Part B*, **3**, 517 (1965).
(13) A. Peterlin, D. T. Turner, and W. Philippoff, *Kolloid Z. Z. Polym.*, **204**, 21 (1965).
(14) A. Peterlin, C. A. Quan, and D. T. Turner, *J. Polym. Sci., Part B*, **3**, 528 (1965).
(15) I. Steg and D. Katz, *J. Appl. Polym. Sci.*, **9**, 3177 (1965).
(16) T. Matsuo, A. Pavan, A. Peterlin, and D. T. Turner, *J. Colloid Interface Sci.*, **24**, 244 (1967).
(17) F. Deveaubois, P. Gramain, and J. Leray, *J. Polym. Sci., Part C*, **16**, 3993 (1968).
(18) P. Munk and A. Peterlin, *Trans. Soc. Rheol.*, **14**, 65 (1970).
(19) F. A. Kanel, Ph.D. Thesis, University of Delaware, Newark, DE, 1972.
(20) F. C. Frank, A. Keller, and M. R. Mackley, *Polymer*, **12**, 467 (1971).
(21) C. L. Sieglaff and K. J. O'Leary, *Trans. Soc. Rheol.*, **14**, 49 (1970).
(22) K. Yamaura, Y. Hoe, S. Matsuzawa, and Y. Go, *Kolloid Z. Z. Polym.*, **243**, 7 (1971).
(23) Z. Laufer, H. L. Jalink, and A. J. Staverman, *J. Polym. Sci., Polym. Chem. Ed.*, **11**, 3005 (1973).
(24) M. R. Mackley and A. Keller, *Polymer*, **14**, 16 (1973).
(25) G. Ver Strate and W. Philippoff, *J. Polym. Sci., Polym. Lett. Ed.*, **12**, 267 (1974).
(26) A. K. Fritzsche and F. P. Price, *Polym. Eng. Sci.*, **14**, 401 (1974).
(27) J. Michele, *Rheol. Acta*, **17**, 42 (1978).
(28) B. A. Wolf, *Makromol. Chem., Rapid Commun.*, **1**, 231 (1980).
(29) A. Y. Malkin, S. G. Kulichikhin, and A. E. Chalykh, *Polymer*, **22**, 1373 (1981).
(30) E. H. Dunlop and L. R. Cox, *Phys. Fluids*, **20** (10), s203 (1977).
(31) C. Rangel-Nafaile, Ph.D. Thesis, University of Delaware, Newark, DE, 1982.
(32) G. Marrucci, *Trans. Soc. Rheol.*, **16**, 321 (1972).
(33) B. A. Wolf, *J. Polym. Sci., Polym. Lett. Ed.*, **18**, 789 (1980).
(34) P. J. Flory, "Principles of Polymer Chemistry", Cornell University Press, Ithaca, NY, 1953.
(35) H. Tompa, "Polymer Solutions", Academic Press, New York, 1956.
(36) W. R. Schowalter, "Mechanics of Non-Newtonian Fluids", Pergamon Press, New York, 1978.
(37) J. E. Frederick, N. W. Tschoegl, and J. D. Ferry, *J. Phys. Chem.*, **68**, 1974 (1964).
(38) G. C. Berry, *J. Chem. Phys.*, **45**, 1338 (1966).
(39) J. D. Ferry, M. L. Williams, and D. M. Stern, *J. Phys. Chem.*, **58**, 987 (1954).
(40) J. D. Ferry, "Viscoelastic Properties of Polymers", 3rd ed., Wiley, New York, 1980, p 315.
(41) T. Kotaka, M. Kurata, and M. Tamura, *Rheol. Acta*, **2**, 179 (1962).
(42) G. Prilutski, R. K. Gupta, T. Sridhar, and M. E. Ryan, *J. Non-Newtonian Fluid Mech.*, **12**, 233 (1983).
(43) R. B. King and A. L. Copley, *Biorheology*, **12**, 355 (1975).
(44) F. B. Hildebrand, "Introduction to Numerical Analysis", McGraw-Hill, New York, 1956, pp 64–8.
(45) A. B. Metzner and A. P. Metzner, *Rheol. Acta*, **9**, 174 (1970).
(46) J. Meissner, *Rheol. Acta*, **10**, 230 (1971).
(47) K. M. Baid and A. B. Metzner, *Trans. Soc. Rheol.*, **21**, 237 (1977).
(48) M. M. Denn, In "The Mechanics of Viscoelastic Fluids", R. Rivlin, Ed., AMD-22, ASME, New York, 1977.
(49) P. K. Agrawal, W. K. Lee, J. M. Lorntson, C. I. Richardson, K. F. Wissbrun, and A. B. Metzner, *Trans. Soc. Rheol.*, **21**, 355 (1977).
(50) D. A. Carey, C. J. Wust, Jr., and D. C. Bogue, *J. Appl. Polym. Sci.*, **25**, 575 (1980). See also R. K. Gupta and A. B. Metzner, *J. Rheol.*, **26**, 181 (1982).
(51) J. L. White and H. Tanaka, *J. Appl. Polym. Sci.*, **26**, 579 (1981).
(52) W. W. Graessley and L. Segal, *Macromolecules*, **2**, 49 (1969).
(53) B. D. Coleman, *Arch. Rat. Mech. Anal.*, **17**, 1, 230 (1964).
(54) C. Truesdell, In "Non-Equilibrium Thermodynamics", R. J. Connelly, R. Herman, and I. Prigogine, Eds., University of Chicago Press, Chicago, 1966, Chapter 6.
(55) G. Astarita and G. Marrucci, "Principles of Non-Newtonian Fluid Mechanics", McGraw-Hill, London, 1974.
(56) R. B. Bird, O. Hassager, R. C. Armstrong, and C. F. Curtiss, "Dynamics of Polymeric Liquids", Vol. 2, Wiley, New York, 1977, p 713.
(57) L. R. G. Treloar, "The Physics of Rubber Elasticity", 3rd ed., Clarendon Press, Oxford, 1975, Chapter 5.